

The Effect of Design and Control Parameters of a Soft Robotic Fish Tail to Maximize Propulsion Force in Undulatory Actuation

Robin Hall, Erik Skorina, Shou-Shan Chiang, and Cagdas D. Onal

Abstract—A tetherless underwater soft robot inspired by the capabilities of biological fish is an ideal tool to navigate complex underwater environments. Such a robot could take dense three-dimensional sensor readings for a better understanding of the ocean’s changing microclimates, while not disturbing the natural underwater life. This paper presents a soft 3D-printed cable-driven flexible fish tail and studies the design and control parameters to maximize its thrust force output for use on a soft robotic fish. The parameters tested were caudal fin shape, fin area, fin thickness, frequency, length of cable retraction, and input waveform. Our results indicate that a 6 in² (38.71 cm²), 2 mm thick trapezoidal tail provides the maximum mean force output with all tested input waveforms. The optimal motor parameters were a triangular input wave with a cable retraction of 16.76 mm operating at 1.67 Hz. Based on our results, using simple driving waveforms with cable driven caudal fins will pave the way towards efficient tetherless exploration and monitoring tasks in complex underwater environments such as coral reefs.

I. INTRODUCTION

The ocean plays a critical role in the world’s economy, biodiversity, and climate regulation. Climate change dramatically threatens this intricate ecosystem [1]. Several impacts include ocean acidification, sea-level rise, deoxygenation, and a world-wide increase in ocean temperature. These effects will be felt all across the world’s oceans, but variable oceanographic conditions create microclimates, small scale marine climates unaffected by greater overlying climate conditions. Current climate associations are analyzed at a resolution of kilometers or more, while most fish experience climate change on the microclimate scale [2]. Temperature data is the primary method of monitoring these, but current methods of temperature data collection lack the resolution required for a nuanced understanding of the impacts of temperature variation on marine species. High resolution temperature data is currently only available through fixed temperature loggers which give researchers limited site-specific data [3]. This paper presents the first stages in the development of a soft robotic fish that will be capable of navigating complex underwater environments and taking dense three-dimensional temperature readings for a better understanding of the ocean’s changing microclimates.

This material is based upon work partially supported by the National Science Foundation (NSF) under Grant Nos. CMMI-1752195, DGE-1922761. Any opinions, findings, and conclusions or recommendations expressed in this material are those of the authors and do not necessarily reflect the views of the NSF.

The authors are with the WPI Soft Robotics Laboratory, Robotics Engineering Department, Worcester Polytechnic Institute, MA 01609, USA. All correspondence should be addressed to Cagdas Onal cdonal@wpi.edu

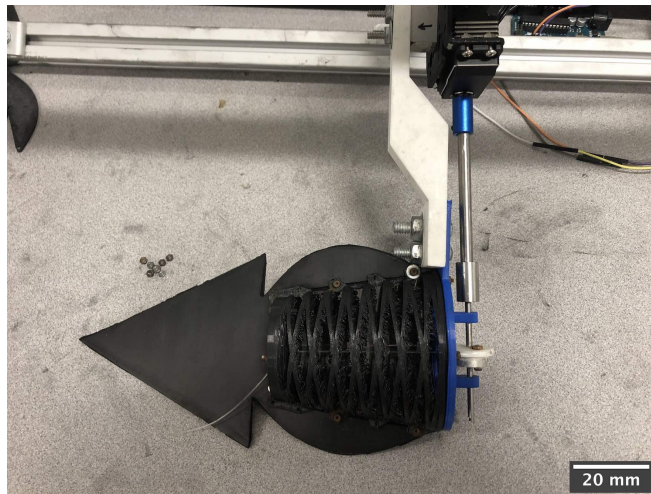


Fig. 1. Wave spring tail with triangular fin mounted in the testing setup. This mount held the tail at a fixed length in the water and enabled us to keep all electronics outside the fish tank.

With the longer-term goal of developing a tetherless and widely accessible soft robotic fish that can monitor temperature variation with very high density without affecting natural underwater life, we propose a cable-actuated 3D-printed wave spring tail that will be used to propel the soft robotic fish via undulatory locomotion. Driven by a servo motor, this wave spring acts like the caudal tail of a fish and has a measurable forward propulsion force [4], [5].

There have been many robotic fish utilizing soft tails as the primary method of undulatory caudal fin actuation with pneumatics or hydraulics [6]–[9]. While these designs have been successful in achieving bioinspired locomotion, they are difficult to manufacture and maintain. Silicone molds must be made, poured, and cured for each half of the tail, then sealed together with a center constraint and tail fin. Finally, the tail is sealed in silicone and pressurized for actuation [7]. Fluidic soft actuators cannot not leak and must also house a complicated gas storage and regulation system.

Compared to robots utilizing pneumatics or hydraulics, our wave spring design required significantly less manual labor and can be almost completely manufactured with a 3D printer capable of printing flexible materials. The tail was 3D-printed with NinjaFlex for easy reproduction and flexibility [10]. Attached to the wave spring tail was a thin rubber caudal fin laser machined in a desired shape, shown in Figure 1. While this design was easy to manufacture, there have been even simpler designs utilizing a single sheet of

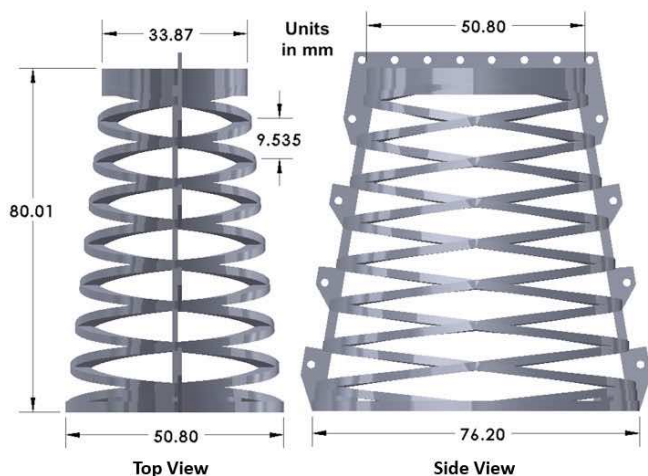


Fig. 2. CAD design of wave spring caudal tail. Mounting holes were utilized to attach different caudal fins on the same tail and driving mechanism.

rubber as a tail fin rotated by a motor [11]. While this did further reduce the manufacturing complexity, it also had a significantly lower force output (less than 1 N) compared to our wave spring tail.

Our design is not the first to utilize cable driven actuation for caudal swimming in a compliant robot [12], [13]. However, many of these designs assemble separate rigid links that are attached on compliant joints. Not only does this increase the manufacturing complexity, but it also takes up unnecessary space and weight. Our tail design was made entirely from soft materials enabling lightweight, inexpensive manufacturing, continuous bending, and easy customizability. To improve the functionality of this design, various motor parameters as well as fin shapes and sizes have been tested to determine the maximum forward force the tail can apply.

The contributions of this work are as follows:

- A customizable cable-driven wave spring fish tail, entirely soft yet selectively stiff.
- A detailed analysis on the effect of motor and physical parameters on fish robot propulsion force.

II. APPROACH AND METHODS

A. Fish Tail Design

We model our soft robotic fish after a biological fish caudal peduncle [14], the tapered region of the fish where the body attaches to the tail fin. This will henceforth be referred to as the “tail”. The robot is intended to operate in a reef environment. Reef fish are morphologically diverse, but share a similar body shape [15]. This body shape was emulated in the tail design, which was a wave spring and shown in Figure 2. The wave spring was a tapered oval consisting of two mirrored helixes, which form a mesh of diamond-shaped cells. These diamond-shaped cells can compress easily, allowing the wave spring to extend or bend as desired. To ensure that the fish tail was only bent laterally, as well as ensure it maintained a fixed length, supports were

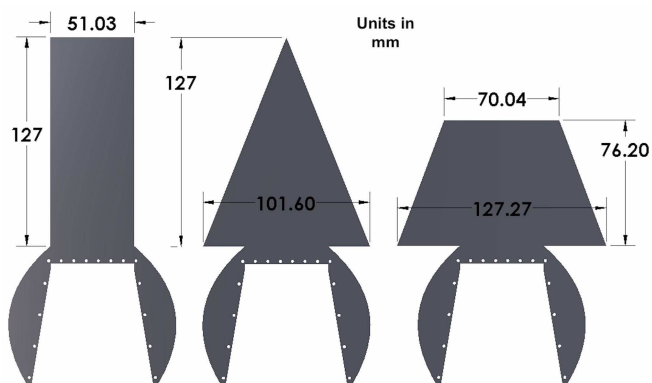


Fig. 3. Base CAD designs for rectangle, triangle and trapezoid fins. For each change in area, only the shape was modified. For each change in thickness, the entire fin was modified.

added on the dorsal and ventral edges of the tail. They resist axial torsion, ensuring that the tip of the wave spring remained aligned with the base. This allowed the fin to mimic the true movement of a biological fish and reduced drag in the other directions. More detail on wave spring structures can be found in [16].

B. Fin Design

The shape of fish tail fins vary dramatically across size, species, and ecosystem. Our goal is to test this robot in a coral reef environment, and in preliminary tests, we used a random selection of reef fish tail fins to model. These shapes proved to be complex and ineffective for accurately assessing other important parameters such as fin thickness and area. For this work, we chose to design fins as regular polygons that simply resembled, not mimicked, biological reef fish. Three shapes were chosen to test; a triangle, rectangle, and trapezoid (Fig. 3). Shapes were selected based on their resemblance to biological fish tail fins [17], [18]. We hypothesized that fin shapes that most closely resembled biological fin shapes would have the highest force output. Each fin was laser machined from sheets of ethylene propylene diene monomer (EPDM) rubber. This rubber had a shore hardness of 60A, while the NinjaFlex used in the wave spring had a shore hardness of 80A. The fins remain stiff enough to keep their shape, but require less stress to deform compared to the wave spring tail. This variable stiffness was an important feature in biologically inspired tail motion [19].

The tail fins primarily generated the forward force of the tail. Along with the three different shapes, three different fin areas and thicknesses were also chosen. The chosen areas were 38.71 cm^2 (6 in^2), 51.61 cm^2 (8 in^2), and 64.52 cm^2 (10 in^2) and the selected thicknesses were 0.5 mm, 1 mm, and 2 mm. Initial testing showed us that fins smaller than 38.71 cm^2 had a significantly lower force response (1.03 N), and fins over 77.42 cm^2 (12 in^2) did not fit in the testing setup and could not be supported by the wave spring tail. Preliminary testing that utilized 0.1 mm thick 3D-printed flexible fins yielded up to 4 times lower average forward force. As a result, no fins thinner than 0.5 mm were included

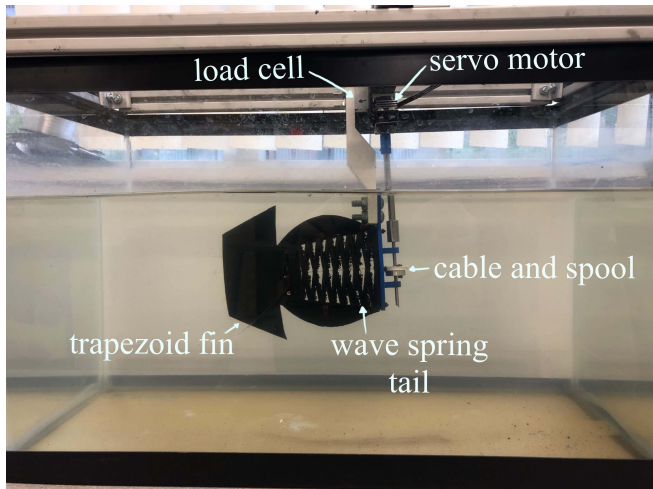


Fig. 4. Testing setup side view with labeled components. The tank was filled with approximately 7.5 gallons of fresh water and the entire tail and cable mechanism was submerged.

in the results. Similar to large area fins, previous experiments that utilized fins thicker than 3 mm proved too heavy for the wave spring tail to support and were similarly not included in the results.

C. Testing Setup

The forward force generated by each different tail configuration was measured on a load cell. The top of the load cell was fixed to an 80/20 brace fitted around a 10 gallon fish tank (Fig. 4). The motor driving the tail was attached to the bottom of the load cell. A plate on the tail was independently connected to the load cell. Without this additional connection, the entire robot would rotate freely without the desired tail deformation. All of the electronics powering and measuring the tail were either suspended above the water or are outside the fish tank. While this does create a force moment, this setup prevented the need to waterproof the design for these tests. For the comparisons being made, this force moment was ignored [20].

The wave spring was attached to a PLA plate which housed the 25.4 mm (1 in) diameter spool used for the cable actuation [21]. The chosen motor was a brushless geared servo motor (A62BHL), which was lightweight (57.2 g) and had a high torque output (20 kg-cm) [22]. It was driven by an Arduino board and a power supply that provided 6.4 volts and 0.3 amps. The motor rotated the spool back and forth between specified angles in the range of -90° and 90° . The cable was a single 24 cm length of monofilament nylon fishing line. Previous iterations used sewing thread and 10 lb fishing line, both of which lost tension or fatigued to failure over time when the motor reached high torques. The cable was connected to each side of the tail fin by a screw used to adjust the tension. As the spool rotated between angles, it pulled the end of the tail, which deformed along the wave spring pattern (see reference video for more details).

Varying the motor input parameters changes the force profile of each fin in different ways. The rotation of the

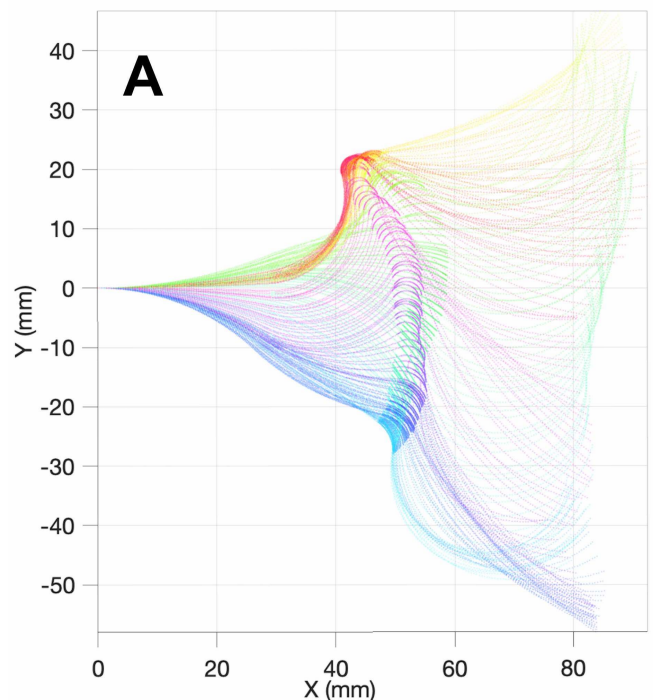


Fig. 5. (A) Tracked shape of 38.71 cm^2 triangle tail for one swimming cycle (0.834 seconds) under the assumption of constant curvature. The color (ROYGBV) corresponds to the chronological progression of the tail. $t = 0 \text{ s}$ corresponds to red and $t = 0.834 \text{ s}$ corresponds to violet. (B) A snapshot of the physical model during the same locomotion experiment with a curve (red) overlaid to indicate the tracked shape. Snapshot taken at $t = 0.004 \text{ s}$.

motor retracted the cable to specified lengths; 14.48 mm, 16.76 mm, and 18.80 mm. These were selected based on the maximum angle (180°) of the servo. It cannot retract the cable greater than 18.80 mm and tests taken with the cable retraction less than 14 mm resulted in continually lower force. Each of these lengths of cable retraction were tested at three frequencies: 1 Hz, 1.25 Hz, and 1.67 Hz. Similar to changes in cable retraction, frequencies lower than 1 Hz resulted in much lower average force (4.36 N). Frequencies greater than 1.67 Hz also resulted in lower average force (5.21 N) as the tail could not reach the maximum length of cable retraction. This relationship led us to believe that cable retraction had a greater impact on force compared to the frequency. Each combination of cable retraction and frequency were implemented in three different ways: a sine wave, a triangle wave, and a square wave. The smooth sine

TABLE I
SUMMARY OF TESTING PARAMETERS

Tail Shapes	Tail Area (cm ²)	Thickness (mm)	Cable Retraction Length (mm)	Frequency (Hz)	Motor Input Wave
Trapezoid	38.71	0.5	14.48	1	Triangle
Triangle	51.61	1	16.76	1.25	Sine
Rectangle	64.52	2	18.80	1.67	Square

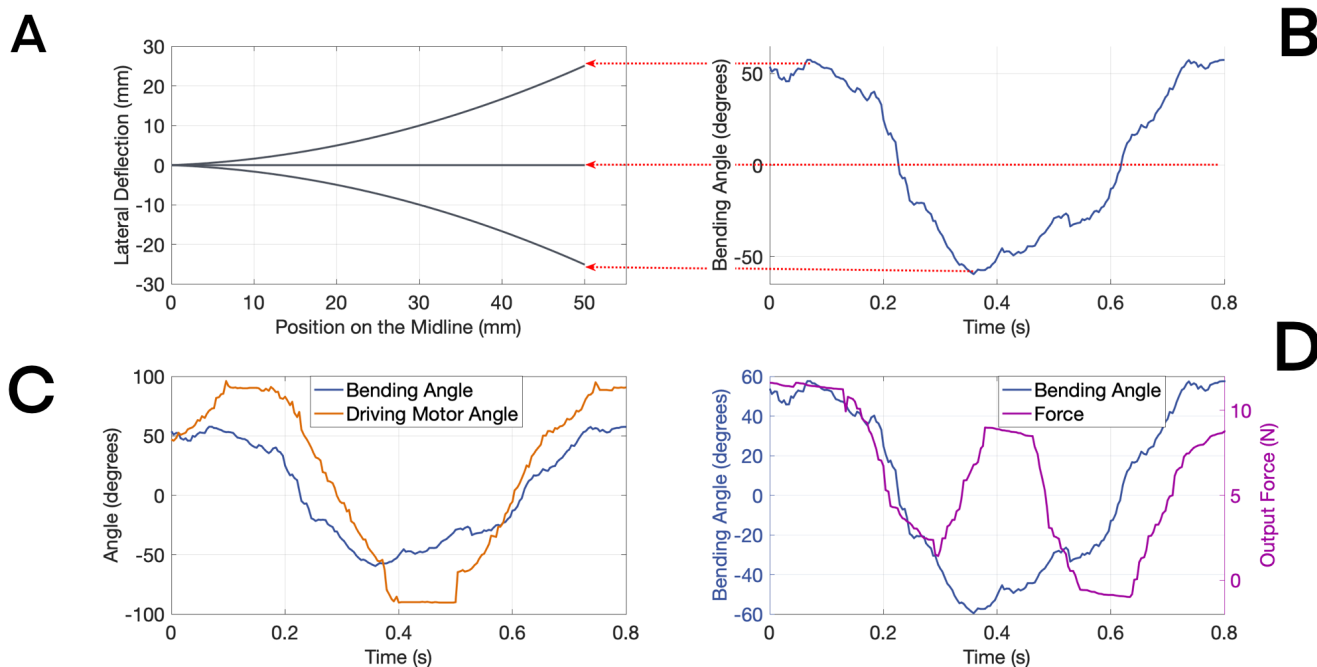


Fig. 6. (A) Lateral deflection of the tip of wave spring tail at its maximum, minimum, and midline bending angle. The motor was operating at 1.67 Hz, cable retraction of 18.80 mm, and a square input wave. (B) Bending angle of the wave spring tail across time and its correspondence with lateral tip deflection. (C) Bending angle of the wave spring tail compared to the driving motor angle from the servo. (D) Bending angle of the wave spring tail compared to the output force of the tail. The fin used was a 38.71 cm², 2 mm thick triangle.

wave more closely resembles the traveling wave motion we were trying to achieve. However, based on our previous work on soft robotic snakes [23], we expect that the square wave would not only reduce the control complexity, but would also produce an accurate biologically inspired traveling wave motion. To facilitate easy testing of a wide variety of tail configurations, attachment points were included along the dorsal and ventral supports on the tail, allowing different fins to be bolted on.

D. Testing

Each physical fin (27 total) was tested with each unique combination of cable retraction, frequency, and input wave resulting in a total of 729 tests. These test parameters are summarized in Table I. During each test, an Arduino board, separate from the one driving the motor, collected values from the load cell for 30 seconds (see reference video). After each combination of motor parameters were tested for an individual fin, the tail was removed from the water, dried, and a new fin was screwed on. This process was repeated for every fin.

E. Tracking Tail Motion

Four points were selected along the length of the tail and fin: at the center and tip of the wave spring module, and then at the start and end of the fin. Tracking each of these points at 240 frames per second, we were able to model the curvature of the tail and fin for one full swimming cycle (Fig. 5A). We assumed constant curvature bending for the tail, and calculated curvatures using the points we tracked. When compared to the physical model, there are some clear differences (Fig. 5B). Many are due to the application of constant curvature on a nonconstant model. We accepted these differences in order to parameterize the tail into notation that is common in soft robotics research [21]. Using this information, we were able to make more comparable observations about the nature of our robot.

III. RESULTS AND DISCUSSION

To examine the behavior of the wave spring tail we started with case studies on a pair of specific parameter combinations, looking at the performance of the tail dur-

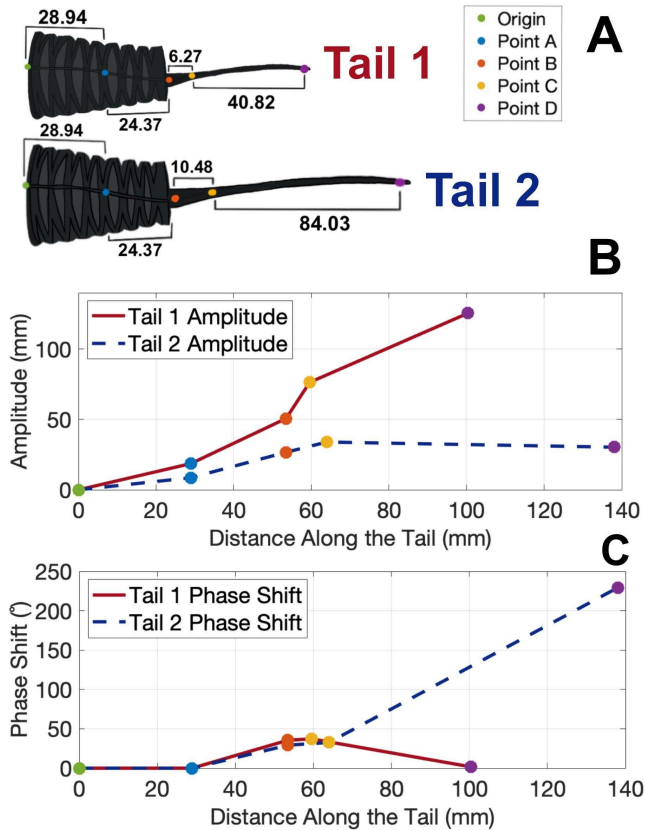


Fig. 7. (A) Tail 1 uses a 38.71 cm^2 triangle fin; Tail 2 uses a 64.52 cm^2 triangle tail. Four points are spaced along the length of the tail at identical locations for each tail. (B+C) Amplitude and phase shift for four discrete points are plotted versus their location along the length of the tail.

ing locomotion. We then examined the effect of parameter changes on the average force output. In general, we expected the design parameters that more closely resembled biology would have a greater force output.

A. Motion Analysis Case Studies

We focused on a single set of parameters, performing position tracking and force analysis on a 38.71 cm^2 , 2 mm thick triangular fin driven by a 1.67 Hz square wave with 18.8 mm cable retraction. The results of these experiments can be seen in Figure 6, where PHYSLET TRACKER was used to determine the exact position of the tail and fin over time.

We were able to calculate the maximum tip deflection to be $\pm 25 \text{ mm}$ (Fig. 6A). Using the same data, we were also able to calculate the bending angle of the wave spring tail (Fig. 6B), resulting in a maximum bending angle of $+57.69^\circ$ and -55.56° . This bending angle was also compared to the driving motor's angle, which has a maximum angle of $\pm 90^\circ$ (Fig. 6C). Finally, in each test, the force output has a similarly sinusoidal nature. As the tail reached its maximum bend angle, the force approached a relative peak (Fig. 6D). As the tail approached the midline, the force approached 0 N.

With the same points used to make the curvature model,

we were able to calculate the amplitude and phase shift along the length of the tail to show the traveling wave that propagates down the length of the tail during locomotion. We compared the performance of two triangular fins, one with an area of 38.71 cm^2 (Tail 1) and the other with an area of 64.52 cm^2 (Tail 2), shown in Figure 7. The tracking points were arranged at the same length fraction along the two fins, taking into account their differing lengths. We found that the traveling wave increased in amplitude along the length of Tail 1, while it leveled off with Tail 2, likely being too big to be effectively driven by the current wave spring.

In biological undulatory motion, the amplitude of the traveling wave increases down the length of the body [24]. Thus, we would expect Tail 1, which has a traveling wave that also increases in amplitude, to have a stronger force output. This agrees with our experimental results, where we found that Tail 1 produced an average of 5.45 N of force, while Tail 2 produced an average of 4.23 N.

B. Parameter Force Analysis

We tested all combinations of the parameters shown in Table I and calculated the average force output for each with the objective of determining the best set of parameters for use on a future soft robotic fish. Each test was inputted into MATLAB and for each, the average force over the runtime of the tests was calculated. The average force for each tail was compared individually. Certain parameters had more of an effect on the thrust force than others. Their correlation was quantified in Table II. This analysis verified one of our original hypotheses; cable retraction had a larger impact on force compared to the frequency.

The trapezoid and triangle fin shapes both produced high force outputs. We previously posited that the design parameters that most accurately resembled biology would produce higher force. We have empirically shown that the trapezoidal fin, which most accurately resembled biological fin shapes, produced the greatest force output in 78% of the tests. The rectangle fins on the other hand, never produced a maximum force output in any test. The trapezoid fin with an area of 38.71 cm^2 and a thickness of 2 mm combined for the best overall force profile for every input wave. With this combination, each input wave resulted in a force over 6 N, the only parameter combination to achieve this mark. Other fin shapes using this combination of area and thickness also yielded high force outputs, notably 6.44 N from the triangle fin with the square input wave and 5.41 N from the rectangle fin with the triangle input wave. In 93% of the tests, thicker fins yielded higher force outputs, with a small margin of difference between 1 mm and 2 mm thickness. In 56% of the tests, the smallest area, 38.71 cm^2 , resulted in the best force outputs. In 96% of the remaining tests, the fins with 51.61 cm^2 area resulted in the highest force.

Trends emerged upon examining different combinations of cable retraction and frequency versus input wave. A frequency of 1 Hz yielded lower forces than other frequencies at any length of cable retraction 96% of the time. Similarly, a cable retraction of 14.48 mm resulted in lower forces than

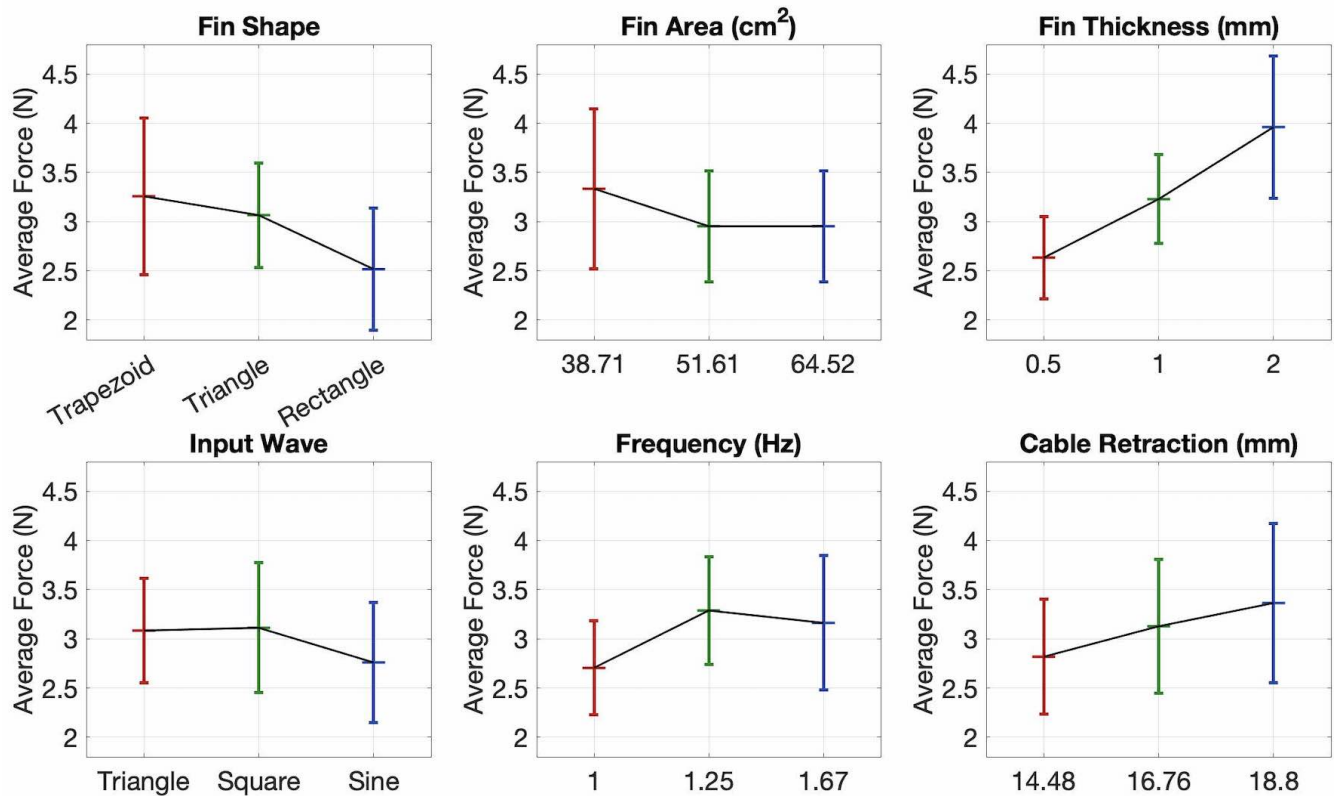


Fig. 8. Trends in force for each parameter. The middle line indicates mean, and error bars plot one standard deviation of variation around the mean.

TABLE II
PARAMETERS CORRELATION TO FORCE

Parameter	Correlation to Force Coefficient
Fin Shape	0.32
Fin Area (cm ²)	-0.25
Fin Thickness (mm)	0.48
Input Wave	0.12
Frequency (Hz)	0.044
Cable Retraction (mm)	0.24

other lengths of cable retraction 92% of the time. Using the triangle input wave, the max force was a result of a 1.67 Hz frequency 84% of the time. The max force of 76% of the tests using the triangle input wave resulted from a 16.76 mm cable retraction. However, when compared to tests using the other input waves, a 16.76 mm cable retraction only resulted in a max force 26% of the time, 7% results from a 14.48 mm cable retraction, and 67% resulted from a 18.80 mm cable retraction. These were mostly from square and sine input waves which both performed very similarly. These results are consistent across both area and thickness. 94% of the tests that resulted in the highest forces using the square and sine input waves were at a 1.25 Hz frequency. The trends of each test parameter was represented in Figure 8

There was one combination of parameters that resulted in the greatest average force output. A 38.71 cm², 2 mm thick trapezoidal fin operating with a triangle input wave and a cable retraction of 16.76 mm at 1.67 Hz yielded an average force of 6.74 N. Since the output force difference between the triangle and square waveforms for the optimal parameter combination was only approximately 0.2 N, it may be desirable to use the much simpler square wave inputs to drive the soft robotic fish. This fin and these parameters will be used as a starting point for the future of the soft robotic fish.

IV. CONCLUSION

With the goal of creating a soft underwater robot inspired by the locomotion capabilities of natural fish, we created a unique and simple cable-driven 3D-printed fish tail. We tested a range of different parameters to find the best fin to use with this tail. It was found that the physical parameters, fin shape, area, and thickness had the most effect over the force. The trapezoid tail shape, 38.71 cm² area, and 2 mm thickness all performed the best. While the motor parameters did not affect the force as much, there were still some that performed better than others. Specifically, a square input wave, 1.25 Hz frequency, and 18.8 mm length of cable retraction all performed better than their counterparts.

The fin shapes used were simplified from their biological counterparts to uniformly measure all other physical parameters. However, the trapezoid fin, which closely resembles

biological fin shapes, did produce a higher force. We would expect that increasing the biological resemblance, such as adding forking (the angle at the center edge of the tail fin seen in many open ocean fish [17]) will improve the performance of the robot. The length of cable retraction, frequency, thickness, and area should also be viewed as a starting reference for future tests. A finer scale search should be completed around each parameter to optimize their effectiveness.

Using the constant curvature assumption for the entire tail segment enabled us to model the swimming motion. However, the connection between the wave spring tail and fin acted more like a hinge than a constant curve and the diameter of the tail was also not constant across the arc length. These both decreased the accuracy of the constant curvature calculations. This was the first attempt to model the tail and future work will need to be done in order to more accurately represent the tail's motion. We will also look to create a dynamics model of the entire fish in order to test a variety of parameters in simulation before applying them to the real robot.

This work is the beginning of a much larger project. The broader motivation remains, to create a free swimming biologically inspired soft fish robot. The next stage of the project will be to move the motor and controller into the fish and include some form of 'skin' over the tail. Sealing the tail is likely to affect the force output and performance of the fish. This will be tested in a similar manner to what was presented here. Other additions will work to reduce the amount of human intervention necessary to operate such a robot, as well as the inclusion of exteroceptive sensors and remote-control applications in a supervision framework. There will also be an investigation into what additional sensing capabilities beyond temperature the robot should have. Ocean acidification and deoxygenation are two factors that could also be examined. These features are important to fully test and quantify in order to maximize the capabilities of the robot.

V. ACKNOWLEDGMENT

The authors thank Dr. Jim Carlton, Dr. Harrison Lane, Mason Mitchell, and Mithulesh Ramkumar, for their assistance in the development and organization of this project. This work was performed at the Worcester Polytechnic Institute Soft Robotics Lab.

REFERENCES

- [1] Jean-Pierre Gattuso, Alexandre K. Magnan, Laurent Bopp, et al. Ocean Solutions to Address Climate Change and Its Effects on Marine Ecosystems. *Frontiers in Marine Science*, 5:337, 2018.
- [2] C. Brock Woodson, Fiorenza Micheli, Charles Boch, Maha Al-Najjar, Antonio Espinoza, Arturo Hernandez, Leonardo Vázquez-Vera, Andrea Saenz-Arroyo, Stephen G. Monismith, and Jorge Torre. Harnessing marine microclimates for climate change adaptation and marine conservation. *Conservation Letters*, 12(2):e12609, 2019.
- [3] Patrick L. Colin and T. M. Shaun Johnston. Measuring Temperature in Coral Reef Environments: Experience, Lessons, and Results from Palau. *Journal of Marine Science and Engineering*, 8(9):680, September 2020.
- [4] M. Sfakiotakis, D.M. Lane, and J.B.C. Davies. Review of fish swimming modes for aquatic locomotion. *IEEE Journal of Oceanic Engineering*, 24(2):237–252, April 1999.
- [5] Ziyu Ren, Kainan Hu, Tianmiao Wang, and Li Wen. Investigation of Fish Caudal Fin Locomotion Using a Bio-Inspired Robotic Model. *International Journal of Advanced Robotic Systems*, 13(3):87, May 2016.
- [6] Ardian Jusufi, Daniel M. Vogt, Robert J. Wood, and George V. Lauder. Undulatory Swimming Performance and Body Stiffness Modulation in a Soft Robotic Fish-Inspired Physical Model. *Soft Robotics*, 4(3):202–210, September 2017.
- [7] Andrew D. Marchese, Cagdas D. Onal, and Daniela Rus. Autonomous Soft Robotic Fish Capable of Escape Maneuvers Using Fluidic Elastomer Actuators. *Soft Robotics*, 1(1):75–87, March 2014.
- [8] Andrew D. Marchese, Robert K. Katzschmann, and Daniela Rus. A Recipe for Soft Fluidic Elastomer Robots. *Soft Robotics*, 2(1):7–25, March 2015.
- [9] Andrew Hess, Xiaobo Tan, and Tong Gao. CFD-based multi-objective controller optimization for soft robotic fish with muscle-like actuation. *Bioinspiration & Biomimetics*, 15(3):035004, March 2020.
- [10] T. J. Wallin, J. Pikul, and R. F. Shepherd. 3D printing of soft robotic systems. *Nature Reviews Materials*, 3(6):84–100, June 2018.
- [11] Yuanhao Zhang, Rongjie Kang, Donato Romano, Paolo Dario, and Zhibin Song. Experimental Research on the Coupling Relationship between Fishtail Stiffness and Undulatory Frequency. *Machines*, 10(3):182, March 2022.
- [12] Yong Zhong, Zheng Li, and Ruxu Du. A Novel Robot Fish With Wire-Driven Active Body and Compliant Tail. *IEEE/ASME Transactions on Mechatronics*, 22(4):1633–1643, August 2017.
- [13] Bingxing Chen and Hongzhou Jiang. Swimming Performance of a Tensegrity Robotic Fish. *Soft Robotics*, 6(4):520–531, August 2019.
- [14] Ziyu Ren, Xingbang Yang, Tianmiao Wang, and Li Wen. Hydrodynamics of a robotic fish tail: Effects of the caudal peduncle, fin ray motions and the flow speed. *Bioinspiration & Biomimetics*, 11(1):016008, February 2016.
- [15] Thomas Claverie and Peter C. Wainwright. A Morphospace for Reef Fishes: Elongation Is the Dominant Axis of Body Shape Evolution. *PLOS ONE*, 9(11):e112732, November 2014.
- [16] Erik H. Skorina and Cagdas D. Onal. Soft Hybrid Wave Spring Actuators. *Advanced Intelligent Systems*, 2(1):1900097, 2020.
- [17] Arun Krishnadas, Santhosh Ravichandran, and Prabhu Rajagopal. Analysis of biomimetic caudal fin shapes for optimal propulsive efficiency. *Ocean Engineering*, 153:132–142, April 2018.
- [18] Alasdair Edwards, Anthony Gill, and Percy Abohweyere. A Revision of Irvine's Marine Fishes of Tropical West Africa. January 2001.
- [19] Anthony J. Clark, Xiaobo Tan, and Philip K. McKinley. Evolutionary multiobjective design of a flexible caudal fin for robotic fish. 10(6):065006, November 2015.
- [20] Hyung-Soo Kim, Jang-Yeob Lee, Won-Shik Chu, and Sung-Hoon Ahn. Design and Fabrication of Soft Morphing Ray Propulsor: Undulator and Oscillator. *Soft Robotics*, 4(1):49–60, March 2017.
- [21] Junius Santoso, Erik H. Skorina, Ming Luo, RuiBo Yan, and Cagdas D. Onal. Design and analysis of an origami continuum manipulation module with torsional strength. In *2017 IEEE/RSJ International Conference on Intelligent Robots and Systems (IROS)*, pages 2098–2104, September 2017.
- [22] Wenyu Zuo, Alicia Keow, and Zheng Chen. Three-Dimensionally Maneuverable Robotic Fish Enabled by Servo Motor and Water Electrolyser. In *2019 International Conference on Robotics and Automation (ICRA)*, pages 4667–4673, May 2019.
- [23] Zhenyu Wan, Yinan Sun, Yun Qin, Erik H. Skorina, Renato Gasoto, Ming Luo, Jie Fu, and Cagdas D. Onal. Design, analysis, and real time simulation of a 3d soft robotic snake. *Soft Robotics*, 2022 (in press).
- [24] Gary B. Gillis. Undulatory Locomotion in Elongate Aquatic Vertebrates: Anguilliform Swimming since Sir James Gray. *American Zoologist*, 36(6):656–665, December 1996.